Thiorphan and *retro*-Thiorphan Display Equivalent Interactions When Bound to Crystalline Thermolysin†

S. L. Roderick,‡ M. C. Fournie-Zaluski,§ B. P. Roques,§ and B. W. Matthews*,‡

Institute of Molecular Biology and Department of Physics, University of Oregon, Eugene, Oregon 97403, and Departement de Chimie Organique, UA 498 CNRS, U 266 INSERM, U.E.R. des Sciences Pharmaceutiques et Biologiques, 4 Avenue de l'Observatoire, 75006 Paris, France

Received August 16, 1988; Revised Manuscript Received October 6, 1988

ABSTRACT: The three-dimensional structures of (*S*)-thiorphan and (*R*)-*retro*-thiorphan bound to thermolysin have been determined crystallographically and refined to residuals of 0.183 and 0.187 at 1.7-Å resolution. Thiorphan [*N*-[(*S*)-2-(mercaptomethyl)-1-oxo-3-phenylpropyl]glycine] [$HSCH_2CH(CH_2C_6H_5)CONHCH_2COOH$] and *retro*-thiorphan [[[(*R*)-1-(mercaptomethyl)-2-phenylethyl]amino]-3-oxopropanoic acid] [$HSCH_2CH(CH_2C_6H_5)NHCOCH_2COOH$] are isomeric thiol-containing inhibitors of endopeptidase EC 24-11 (also called "enkephalinase"). The mode of binding of thiorphan to thermolysin is similar to that of (2-benzyl-3-mercaptopropanoyl)-L-alanylglycinamide [Monzingo, A. F., & Matthews, B. W. (1982) *Biochemistry 21*, 3390–3394] with the inhibitor sulfur atom coordinated to the active site zinc and the peptide portion forming substrate-like interactions with the enzyme. The isomeric inhibitor *retro*-thiorphan, which differs from thiorphan by the inversion of an amide bond, utilizes very similar interactions with enzyme. Despite the inversion of the –CO–NH– linkage the carbonyl oxygen and amide nitrogen display very similar hydrogen bonding, as anticipated by B. P. Roques et al. [(1983) *Proc. Natl. Acad. Sci. U.S.A. 80*, 3178–3182]. These results explain why thermolysin and possibly other zinc endopeptidases such as endopeptidase EC 24-11 fail to discriminate between these retro–inverso inhibitors.

Thermolysin is a heat-stable zinc endopeptidase, M_r 34 600, isolated from *Bacillus thermoproteolyticus*. Its three-dimensional structure has been determined, and an catalytic mechanism based on the structure of various thermolysin–inhibitor complexes has been proposed (Weaver et al., 1977; Kester & Matthews, 1977; Holmes & Matthews, 1981; Hangauer et al., 1984; Holden et al., 1987; Matthews, 1988).

One class of tight-binding reversible inhibitors of the zinc peptidases are substrate analogue mercaptans (Cushman et al., 1977; Ondetti et al., 1977, 1979; Nishino & Powers, 1979; Patchett et al., 1980; Harris et al., 1981; Maycock et al., 1981). Captopril, the well-known antihypertensive drug, is the prototypical example. The structure of a thermolysin complex with (2-benzyl-3-mercaptopropanoyl)-L-alanylglycinamide (BAG) [$HSCH_2CH(CH_2C_6H_5)CONHCH(CH_3)CONHCH_2CONH_2$] has been determined and demonstrates distorted tetrahedral coordination of the inhibitor sulfur atom to the active site zinc and substrate-like interactions of the peptide moiety with side chains of the enzyme (Monzingo & Matthews, 1982).

Recently, Roques and co-workers (Roques et al., 1980, 1983) have studied mercaptan-induced inhibition of "endopeptidase EC 24-11" (also called "enkephalinase") (EC 3.4.24.11) a neutral zinc endopeptidase responsible for cleaving the Gly–Phe bond of enkephalins, endogenous morphine-like pentapeptides. Inhibitors of this enzyme are of considerable therapeutic value and may serve as functional probes of the analgesic response (Roques & Fournie-Zaluski, 1986). Taking into account the substate specificities of endopeptidase 24-11 and the ability of the active site zinc atom to coordinate a thiol group, the tight-binding mercaptan inhibitor thiorphan was designed and synthesized (Roques et al., 1980). Although this inhibitor binds tightly to enkephalinase (K_i = 1.9 nM), it also binds to angiotensin-converting enzyme, a zinc peptidase involved in the regulation of blood pressure (K_i = 140 nM). In an effort to design a more selective inhibitor, the isomer containing a retro–inverso amide bond, *retro*-thiorphan, was prepared (Roques et al., 1983). This compound binds to endopeptidase 24-11 nearly as well as thiorphan (K_i = 2.3 nM) but offers complete selectivity against the angiotensin-converting enzyme (K_i > 10 000 nM).

Amino acid sequence analysis suggests that endopeptidase 24-11 and thermolysin may have several active site residues in common (Devault et al., 1987; Malfroy et al., 1987; Benchetrit et al., 1988). Biochemical experiments and binding studies, using separate *R* and *S* isomers of thiorphan and *retro*-thiorphan (Fournie-Zaluski et al., 1986) indicate that the substrate specificities of these enzymes are very similar (Kerr & Kenny, 1974; Beaumont & Roques, 1986; Benchetrit et al., 1987). In particular, thermolysin also fails to discriminate between (*S*)-thiorphan and (*R*)-*retro*-thiorphan although thermolysin binds these compounds much less tightly than enkephalinase [K_i = 1.8 μM for (*S*)-thiorphan; K_i = 2.3 μM for (*R*)-*retro*-thiorphan; Benchetrit et al., 1987].

Because of these similarities between endopeptidase 24-11 and thermolysin, it was of interest to determine the three-dimensional structure of these thermolysin–thiorphan and –*retro*-thiorphan complexes as a model of their mode of binding of enkephalinase. In particular, this study addresses the question of how an inhibitor amide bond containing atoms that form important interactions with the enzyme can be inverted yet have almost no effect on the affinity of binding.

Materials and Methods

Thermolysin was obtained from Calbiochem and crystallized as described by Colman et al. (1972). The crystals are stored

† This work was supported in part by grants from the National Science Foundation (DMB 8611084), from the National Institutes of Health (GM 20066), and from the Lucille P. Markey Charitable Trust (to B.W.M.).

* Address correspondence to this author at the Institute of Molecular Biology, University of Oregon, Eugene, OR 97403.

‡ University of Oregon.

§ U.E.R. des Sciences Pharmaceutiques et Biologiques.

0006-2960/89/0428-1493$01.50/0

Table I: Intensity Statistics for Thermolysin–Inhibitor Complexes[a]

	(*S*)-thiorphan	(*R*)-*retro*-thiorphan
number of films	23	25
average R_{sym} (%)	3.8	3.2
average R_{sca} (%)	2.4	2.0
R_{merge} (%)	9.8	5.8
total reflections measured	55 461	78 234
independent reflections	26 142	27 574
resolution (Å)	1.7	1.7
average isomorphous difference (%)	13.6	10.8
cell dimensions		
a, *b* (Å)	94.0	94.0
c (Å)	132.1	132.0

[a] R_{sym} measures the agreement between symmetry-related reflections on the same film, R_{sca} measures the agreement between reflections recorded on successive films in a given film pack, and R_{merge} gives the overall agreement between intensities measured on different films.

in mother liquor containing 0.01 M Tris (acetate), 0.01 M calcium acetate, and 7% dimethyl sulfoxide (v/v), pH 7.2 at 4 °C, prior to use.

Native crystals were soaked in mother liquor containing 4 mM dithiothreitol and various concentrations of inhibitor at 4 °C. In order to screen for optimal conditions, precession photographs of the (*h0l*) zone were recorded and used to calculate difference Fourier maps. An example of such a map is included in Holden and Matthews (1987). These preliminary studies indicated a binding site for the electron-dense sulfur atom close to the active site zinc. The inhibitor concentration and time of soak used to prepare crystals for three-dimensional data collection were 0.25 mM thiorphan for 5 days and 0.50 mM *retro*-thiorphan for 14 days.

Three-dimensional X-ray diffraction data were measured to 1.7-Å resolution by using oscillation photography (Schmid et al., 1981). The complex crystals, space group $P6_122$, were rotated 1.2° about the *c* axis during each 5–6-h exposure for a net rotation of about 30°. The X-ray source was an Elliott GX-21 rotating-anode generator operated at 39 kV and 110 mA and employing a graphite monochromator and collimating slits near the crystal. The intensity statistics for the diffraction data are summarized in Table I.

Electron density maps for model building were calculated by using amplitudes $2F_{complex,obsd} - F_{calcd}$, where the calculated structure factor and phases corresponded to the refined atomic coordinates (Holmes & Matthews, 1982) with active site solvent atoms removed (Figure 1). The preliminary atomic coordinates obtained from the maps were refined with data to 1.7-Å resolution with the "TNT" program package utilizing the restrained least-squares method (Tronrud et al., 1987). The final crystallographic *R* values for thiorphan and *retro*-thiorphan complex structures were 18.3% and 18.7%, respectively. The refined inhibitor coordinates are listed in Table II and have an estimated uncertainty of 0.15 Å. Refinement statistics and deviation of the final models from "ideal" geometry are shown in Table III.

Results

The refined models of thiorphan and *retro*-thiorphan in the extended thermolysin active site are shown in Figure 2. The conformation of thiorphan bound to thermolysin is very similar to that determined for the thermolysin–BAG complex (Monzingo & Matthews, 1982) as was anticipated on the basis of their structural similarity. As observed in a variety of thermolysin–inhibitor structures, the phenyl ring of the inhibitor binds in the S_1' hydrophobic specificity pocket (Weaver et al., 1977; Kester & Matthews, 1977; Holmes & Matthews, 1981). The sulfur atom of each inhibitor, presumably in the anionic form, is coordinated to the active site zinc with distorted tetrahedral geometry. The zinc–sulfur interatomic distances in the two complexes are 2.4 and 2.3 Å, respectively. Details of the zinc–ligand geometry are given in Table IV.

The close interatomic distances between the respective inhibitors and the enzyme are listed in Table V (see also Figures 3 and 4). The amide or (retro-amide) carboxyl oxygen of both inhibitors lies within hydrogen bonding distance of the NEE1 and NEE2 atoms of Arg 203 in the thiorphan and *retro*-thiorphan complexes. The distances between the presumed

Table II: Inhibitor Coordinates[a]

atom	*x*	*y*	*z*	*B*
		(*S*)-Thiorphan		
SG	52.5	18.9	−6.7	28.8
CB2	51.7	18.5	−5.1	21.1
CA	52.8	18.4	−4.0	25.8
CB1	52.0	18.7	−2.8	26.5
CG	53.1	18.7	−1.7	23.1
CD1	54.2	19.5	−1.9	21.9
CD2	52.8	17.9	−0.6	23.1
CE1	55.2	19.5	−0.9	24.6
CE2	53.8	18.0	0.4	20.5
CZ	55.0	18.8	0.2	30.7
C	53.7	17.1	−3.9	20.9
O	54.9	17.0	−3.8	21.1
N	52.9	16.0	−3.8	20.9
CA	53.3	14.6	−3.8	20.3
C	52.6	13.9	−5.0	25.8
O	51.6	14.4	−5.5	27.6
O	53.1	12.8	−5.4	37.9
		(*R*)-*retro*-Thiorphan		
SG	52.5	19.0	−6.8	26.1
CB2	51.6	19.1	−5.2	20.0
CA	52.6	18.6	−4.1	23.8
CB1	52.1	19.2	−2.8	23.4
CG	53.1	18.9	−1.7	20.2
CD1	54.3	19.5	−1.7	23.0
CD2	52.7	18.1	−0.6	22.3
CE1	55.2	19.3	−0.7	26.2
CE2	53.6	17.8	0.4	23.6
CZ	54.9	18.5	0.4	27.3
N	52.5	17.1	−3.9	30.8
C	53.6	16.4	−3.7	23.3
O	54.8	16.8	−3.7	20.0
CA	53.3	14.8	−3.4	22.2
C	52.8	14.1	−4.7	28.3
O	51.9	14.6	−5.5	31.8
O	53.4	13.0	−4.9	42.5

[a] Coordinates (*xyz*) are in angstroms (Å) in the standard orthogonal thermolysin coordinate frame (Holmes & Matthews, 1982). The crystallographic thermal factor *B* is in Å^2. The complete sets of thermolysin–inhibitor complexes have been deposited in the Brookhaven Data Bank.

Table III: Refinement Statistics for Thermolysin–Inhibitor Complexes

	(*S*)-thiorphan	(*R*)-*retro*-thiorphan
resolution limits (Å)	10.0–1.7	10.0–1.7
initial *R* factor (%)[a]	24.5	24.8
final *R* factor (%)	18.3	18.7
number of cycles	35	40
number of reflections used	25 988	27 376
number of atoms	2615	2615
rms deviations from ideality		
bond length (Å)	0.023	0.024
bond angle (deg)	3.5	3.3
planarity (trigonal) (Å)	0.013	0.014
planarity (other planes) (Å)	0.015	0.017
torsion angle (deg)[b]	23.7	23.7

[a] R factor $= \sum|F_{obsd} - F_{calcd}|/\sum F_{obsd}$. [b] The torsion angles refer to the rotations of side chains about single bonds. These rotations were not restrained during refinement.

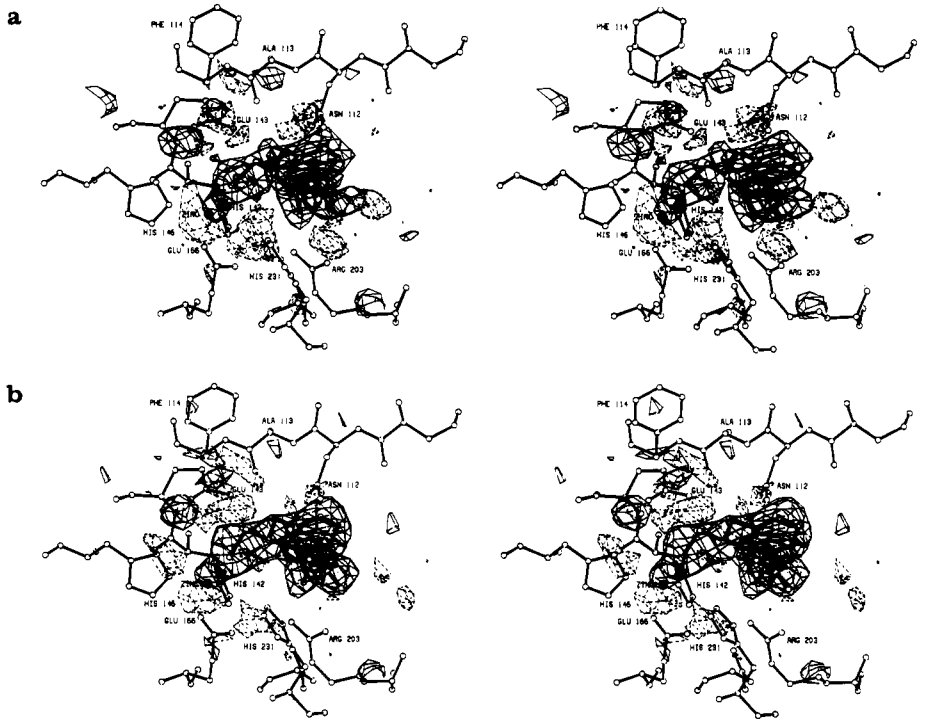

FIGURE 1: Electron density maps at 1.9-Å resolution showing the difference between inhibited and native thermolysin. Amplitudes $F_{complex} - F_{calcd}$ were used, where the calculated amplitudes and the phases correspond to refined native thermolysin with water molecules removed from the active site region. The superimposed inhibitor is drawn with thick bonds. Contours were drawn at 2.5σ and -2.5σ, where σ is the root mean square electron density throughout the unit cell. (a) (*S*)-Thiorphan; (b) (*R*)-*retro*-thiorphan.

Table IV: Zinc–Ligand Geometry

	distance (Å)	
ligand	(*S*)-thiorphan	(*R*)-*retro*-thiorphan
His 142 NE2	2.1	2.1
His 146 NE2	2.1	2.0
Glu 166 OE1	2.0	2.2
inhibitor S	2.4	2.3
	angle (deg)	
ligands	(*S*)-thiorphan	(*R*)-*retro*-thiorphan
S–Zn–NE2 (His 142)	116.3	119.1
S–Zn–NE2 (His 146)	112.8	114.1
S–Zn–OE1 (Glu 166)	101.7	100.7

Table V: Selected Thermolysin–Inhibitor Distances

		distance (Å)				
		(*S*)-thiorphan		(*R*)-*retro*-thiorphan		
protein atom	inhibitor atom	exptl[a]	model building[a]	exptl[a]	model building[a]	BAG[b]
Asn 112 OD1	Gly N	3.1	2.9	3.0	2.9	3.1
Asn 112 ND2	Gly O	3.0	3.0	3.2	3.0	2.9
Arg 203 NEE1	ψ-Phe O	2.8	3.2	2.9	3.3	2.9
Arg 203 NEE2	ψ-Phe O	2.8	3.3	2.9	3.0	2.8

[a] The experimental values are from the present work. The values from model building were obtained by Benchetrit et al. (1987). [b] BAG is (2-benzyl-3-mercaptopropanoyl)-L-alanylaglycinamide (Monzingo & Matthews, 1982).

OD1 of Asn 112 to the inhibitor amide nitrogen in both complexes are very similar despite the fact that these amide nitrogen atoms occupy positions separated by 1.2 Å (Table V). These distances as well as the distances between the ND2 atom of Asn 112 and the terminal carboxylate oxygen indicate somewhat longer and weaker interactions than the hydrogen bonds involving Arg 203 and the amide carboxyl oxygen.

The distance between the CB2 atom of the pseudophenylalanine side chain of *retro*-thiorphan and the OE1 atom of Glu 143 is 2.7 Å, which is among the closest van der Waals contact distances in the two complexes. The corresponding distances in the thiorphan and previously determined BAG complex structures are 2.9 and 3.0 Å. This contact apparently pushes the side chain of Glu 143 away in the *retro*-thiorphan complex as indicated by the pattern of positive and negative difference electron density above and below the side-chain carboxylate group of this residue (Figure 1) and the refined coordinates of the side-chain atoms (Figure 3).

Discussion

Rational design based on substrate analogue mercaptans has proven to be an effective means by which tight-binding inhibitors of the zinc peptidases can be obtained. These inhibitors contain a thiol group that coordinates with the zinc atom of the enzyme and a peptide moiety that mimics a natural substrate. The binding specificity of mercaptan inhibitors can be altered within this framework by changing side-chain types, overall peptide length, and the type of terminal blocking groups used, if any. However, it has been difficult to design potent and highly selective inhibitors of enkephalinase by employing these methods. For example, inhibitors with methylated amide bonds or carboxy-terminal proline residues often reduce the inhibitory potency toward enkephalinase without significant effect on other zinc peptidases such as the angiotensin-converting enzyme (Fournie-Zaluski et al., 1980). The retro-amide analogue *retro*-thiorphan represents an attempt to design a specific and potent inhibitor of enkephalinase according to a rationale based on substrate analogue mercaptans (Roques et al., 1983).

The three-dimensional structures of the isomeric mercaptans thiorphan and *retro*-thiorphan bound to thermolysin demonstrate that indeed both compounds bind to thermolysin through sulfur–zinc coordination and hydrophobic interactions in the S_1' hydrophobic specificity pocket expected of substrate–

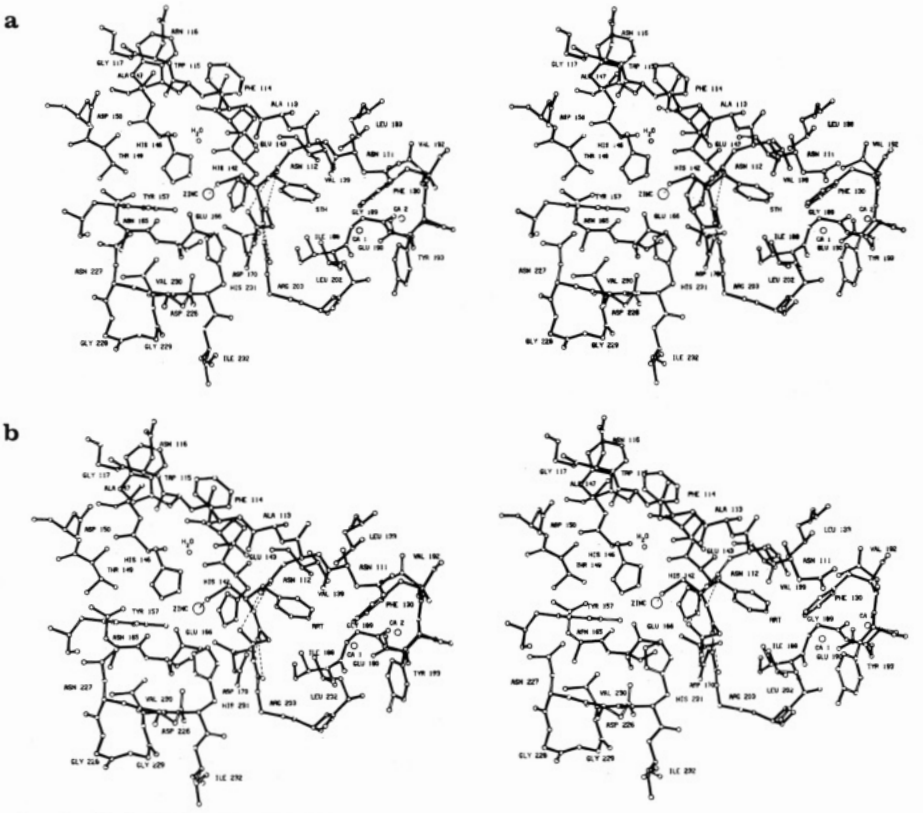

FIGURE 2: Stereoviews showing the inhibitors bound in the extended thermolysin active site. Interactions between the inhibitors and the enzyme are drawn as broken lines. (a) (*S*)-Thiorphan (STH); (b) (*R*)-*retro*-thiorphan (RRT).

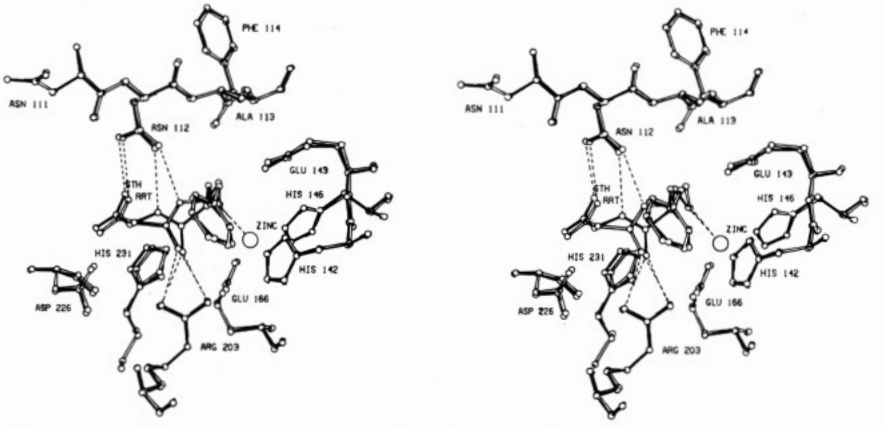

FIGURE 3: Superposition of the two enzyme–inhibitor complexes showing the equivalence of their hydrogen-bonding and other interactions. The complex of thermolysin with (*S*)-thiorphan is drawn with solid bonds; that with (*R*)-*retro*-thiorphan is drawn with open bonds.

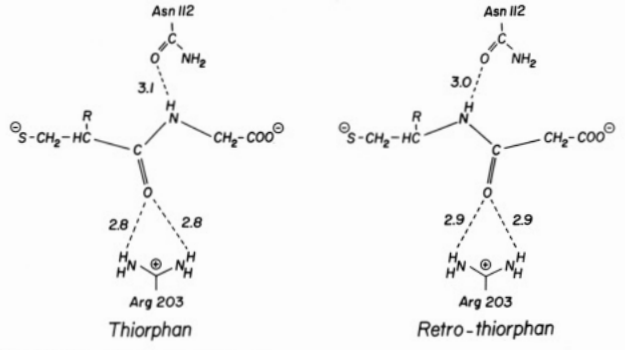

FIGURE 4: Schematic illustration showing how the inversion of the amide bond leaves the enzyme–inhibitor hydrogen bond lengths almost invariant.

analogue mercaptans. The maintenance of these interactions as well as the hydrogen bonds involving the inhibitor and enzyme side chains in both complexes is consistent with the similar binding affinities of these compounds to thermolysin.

It was hypothesized that the replacement of a normal amide bond in thiorphan by a retro-amide bond in *retro*-thiorphan would allow the respective groups to maintain similar interactions with the enzyme [see Figure 1 of Roques et al. (1983)]. This idea was explored further (Benchetrit et al., 1987) by building models of the respective inhibitors in the active site of thermolysin using the known coordinates of the BAG–thermolysin complex (Monzingo & Matthews, 1982) as a starting point. Some enzyme–inhibitor distances obtained from this model-building exercise are included in Table V and can be compared with the experimental values. The agreement is striking. Also, as was anticipated by the model building, the carbonyl oxygen and the amide nitrogen of the amide and the retro-amide groups display essentially equivalent hydrogen bonding interactions with Arg 203 and Asn 112 (Figures 3 and 4; Table V).

There are reasons to think that binding of thiorphan and *retro*-thiorphan to enkephalinase may have similarities to their observed binding to thermolysin. Although enkephalinase binds these inhibitors much more tightly than does thermolysin, this is in part due to the preference of endopeptidase 24-11 for substrates bearing free carboxy-terminal groups such as its natural pentapeptide substrates (Fournie-Zaluski et al., 1980). The possible amino acid sequence correspondence between these enzymes (Devault et al., 1987; Malfroy et al., 1987; Benchetrit et al., 1988), the similarity of their enzymatic activities (Kerr & Kenny, 1974; Beaumont & Roques, 1986; Benchetrit et al., 1987), and their similar lack of discrimination between thiorphan and *retro*-thiorphan collectively argue for similar modes of binding of these inhibitors to both thermolysin and enkephalinase.

The hypothesis is supported by site-directed mutagenesis of endopeptidase 24-11 (Devault et al., 1988a,b). The replacement of Glu 584 with Asp or Val completely abolished the hydrolyzing activity of the recombinant protein but did not modify the binding of a substrate-related hydroxamic acid inhibitor. This residue is the presumed homologue of the catalytically essential residue Glu 143 of thermolysin.

Taken together, these results suggest that the known tertiary structure of thermolysin can be used as a working model for the endopeptidase 24-11 active site, allowing "docking" of inhibitors by computer graphics as recently illustrated in the case of the angiotensin-converting enzyme (Hangauer et al., 1984) and renin (Blundell et al., 1987) inhibitors. The use of these rational molecular approaches should aid the design of new classes of potent, selective, and orally active enkephalinase inhibitors.

Acknowledgments

We thank Drs. Larry Weaver and Dale Tronrud for help with data collection and computational aspects.

References

Beaumont, A., & Roques, B. P. (1986) *Biochem. Biophys. Res. Commun. 139*, 733–739.

Benchetrit, T., Fournie-Zaluski, M. C. & Roques, B. P. (1987) *Biochem. Biophys. Res. Commun. 147*, 1034–1040.

Benchetrit, T., Bissery, V., Mornon, J. P., Devault, A., Crine, P., & Roques, B. P. (1988) *Biochemistry 27*, 592–596.

Blundell, T. L., Sibanda, B. L., Sternberg, M. J. E., & Thornton, J. M. (1987) *Nature 326*, 347–352.

Colman, P. M., Jansonius, J. N., & Matthews, B. W. (1972) *J. Mol. Biol. 70*, 701–724.

Cushman, D. W., Cheung, H. S., Sabo, E. F., & Ondetti, M. A. (1977) *Biochemistry 16*, 5484–5491.

Devault, A., Lazure, C., Nault, C., Le Moual, H., Seidah, N. G., Chretien, M., Kahn, P., Powell, J., Mallet, J., Beaumont, A., Roques, B. P., Crine, P., & Boileau, G. (1987) *EMBO J. 6*, 1317–1322.

Devault, A., Salis, V., Nault, C., Beaumont, A., Roques, B., Crine, P. & Boileau, G. (1988a) *FEBS Lett. 231*, 54–58.

Devault, A., Nault, C., Zollinger, M., Fournie-Zaluski, M. C., Roques, B. P., Crine, P., & Boileau, G. (1988b) *J. Biol. Chem. 263*, 4033–4040.

Fournie-Zaluski, M. C., Llorens, C., Gacel, G., Malfroy, B., Swerts, J. P., Lecomte, J. M., Schwartz, J. C., & Roques, B. P. (1980) in *Proceedings of the Sixteenth European Peptide Symposium* (Brunfeldt, K., Ed.) pp 476–481, Scriptor, Copenhagen.

Fournie-Zaluski, M. C., Lucas-Soroca, E., Devin, J., & Roques, B. P. (1986) *J. Med. Chem. 29*, 751–757.

Hangauer, D. G., Monzingo, A. F., & Matthews, B. W. (1984) *Biochemistry 23*, 5730–5741.

Harris, R. B., Ohlsson, J. T., & Wilson, I. B. (1981) *Arch. Biochem. Biophys. 206*, 105–112.

Holden, H. M., & Matthews, B. W. (1988) *J. Biol. Chem. 263*, 3256–3260.

Holden, H. M., Tronrud, D. E., Monzingo, A. F., Weaver, L. H., & Matthews, B. W. (1987) *Biochemistry 26*, 8542–8553.

Holmes, M. A., & Matthews, B. W. (1981) *Biochemistry 20*, 6912–6920.

Holmes, M. A., & Matthews, B. W. (1982) *J. Mol. Biol. 160*, 623–629.

Kerr, M. A., & Kenny, A. J. (1974) *Biochem. J. 137*, 477–488.

Kester, W. R., & Matthews, B. W. (1977) *Biochemistry 16*, 2506–2516.

Malfroy, B., Schonfield, P. R., Kuang, W. J., Seeburg, P. H., Mason, A. J., & Henzel, W. J. (1987) *Biochem. Biophys. Res. Commun. 144*, 59–66.

Matthews, B. W. (1988) *Acc. Chem. Res. 21*, 333–340.

Maycock, A. L. De Sousa, D. M., Payne, L. G., ten Broeke, J., Wu, M. T., & Patchett, A. A. (1981) *Biochem. Biophys. Res. Commun. 102*, 963–929.

Monzingo, A. F., & Matthews, B. W. (1982) *Biochemistry 21*, 3390–3394.

Nishino, N., & Powers, J. C. (1979) *Biochemistry 18*, 4340–4347.

Ondetti, M. A., Rubin, B., & Cushman, D. W. (1977) *Science (Washington, D.C.) 196*, 441–444.

Ondetti, M. A., Condon, M. E., Reid, J., Sabo, E. F., Cheung, H. S., & Cushman, D. W. (1979) *Biochemistry 18*, 1427–1430.

Patchett, A. A., Harris, E., Tristram, E. W., Wyvratt, M. J., Wu, M. T., Taub, D., Peterson, E. R., Ikeler, T. J., ten Broeke, J., Payne, L. G., Ondeyka, D. L., Thorsett, E. D., Greenlee, W. J., Lohr, N. S., Hoffsommer, R. D., Joshua, H., Ruyle, W. V., Rothrock, J. W., Aster, S. D., Maycock, A. L., Robinson, F. M., Hirschmann, R., Sweet, C. S., Ulm, E. H., Gross, D. M., Vassil, T. C., & Stone, C. A. (1980) *Nature (London) 288*, 280–283.

Roques, B. P., & Fournie-Zaluski, M. C. (1986) *NIDA Res. Monogr. Ser. 70*, 128–154.

Roques, B. P., Fournie-Zaluski, M. C., Soroca, E., Lecomte, J. M., Malfroy, B., Llorens, C., & Schwartz, J. C. (1980) *Nature (London) 288*, 286–288.

Roques, B. P., Lucas-Soroca, E., Chaillet, P., Costentin, J., & Fournie-Zaluski, M. C. (1983) *Proc. Natl. Acad. Sci. U.S.A. 80*, 3178–3182.

Schmid, M. F., Weaver, L. H., Holmes, M. A., Grütter, M. G., Ohlendorf, D. H., Reynolds, R. A., Remington, S. J., & Matthews, B. W. (1981) *Acta Crystallogr. A37*, 701–710.

Tronrud, D. E., Ten Eyck, L. F., & Matthews, B. W. (1987) *Acta Crystallogr., Sect. A: Found. Crystallogr. A43*, 489–501.

Weaver, L. W., Kester, W. R., & Matthews, B. W. (1977) *J. Mol. Biol. 114*, 119–132.